Ensemble Simulations of Asian–Australian Monsoon Variability by 11 AGCMs*

BIN WANG

Department of Meteorology and International Pacific Research Center, University of Hawaii at Manoa, Honolulu, Hawaii

IN-SIK KANG AND JUNE-YI LEE

School of Earth and Environmental Sciences, Seoul National University, Seoul, South Korea

(Manuscript received 17 October 2002, in final form 31 January 2003)

ABSTRACT

Ensemble simulations of Asian–Australian monsoon (A–AM) anomalies were evaluated in 11 atmospheric general circulation models for the unprecedented El Niño period of September 1996–August 1998. The models' simulations of anomalous Asian summer rainfall patterns in the A–AM region (30°S–30°N, 40°–160°E) are considerably poorer than in the El Niño region. This is mainly due to a lack of skill over Southeast Asia and the western North Pacific (5°–30°N, 80°–150°E), which is a striking characteristic of all the models. The models' deficiencies result from failing to simulate correctly the relationship between the local summer rainfall and the SST anomalies over the Philippine Sea, the South China Sea, and the Bay of Bengal: the observed rainfall anomalies are negatively correlated with SST anomalies, whereas in nearly all models, the rainfall anomalies are positively correlated with SST anomalies. While the models' physical parameterizations have large uncertainties, this problem is primarily attributed to the experimental design in which the atmosphere is forced to respond passively to the specified SSTs, while in nature the SSTs result in part from the atmospheric forcing.

Regional monsoon dynamic indices are calculated for the Indian, the western North Pacific, and the Australian monsoons, respectively. Most models can realistically reproduce the western North Pacific and Australian monsoon, yet fail with the Indian monsoon. To see whether this is generally the case, a suite of five Seoul National University model runs with the same observed lower boundary forcing (and differing only in their initial conditions) was examined for the period 1950–98. The skill in the 49-yr ensemble simulations of the Indian monsoon is significantly higher than the skill for the period 1996–98. In other words for the unprecedented 1997/98 El Niño period, the models under study experience unusual difficulties in simulating the Indian monsoon circulation anomalies. Moreover, the observed Webster–Yang index shows a decreasing trend over the last 50 yr, a trend missed by the models' ensemble simulations.

1. Introduction

The Asian–Australian monsoon (A–AM) exhibits the strongest annual variation in the global climate system; it interacts with the El Niño–Southern Oscillation (ENSO; Webster et al. 1998) and has a far-reaching impacts on North American (Lau and Weng 2001) and global climate (Webster and Yang 1992). While the A–AM anomalies result from complex atmosphere–ocean–land interactions, ENSO has been recognized as the primary factor determining the interannual variation of the A–AM.

Several previous studies that evaluated the performance of atmospheric general circulation models (AGCMs) have found that the AGCMs generally have little skill in predicting the all-Indian summer rainfall. Sperber and Palmer (1996) showed that 32 models in the Atmospheric Model Intercomparison Project (AMIP) showed little or no predictability in the all-Indian rainfall from 1979 to 1988 except during the 1987 El Niño and the 1988 La Niña. This low predictability was speculated to be due to intrinsic chaotic dynamics associated with intraseasonal monsoon fluctuations and/or unpredictable land surface process interactions. Using the Geophysical Fluid Dynamics Laboratory (GFDL) AGCM, Goswami (1998) suggested an explanation for the poor predictability of Indian precipitation in the model. It was hypothesized that the contribution of ENSO to the interannual variability in this region is comparable to those regional-scale fluctuations arising from an internal oscillation unrelated to SST anomalies.

Better modeling of the Indian summer rainfall has

* School of Ocean and Earth Science and Technology Publication Number 6240 and International Pacific Research Center Publication Number 228.

Corresponding author address: Dr. Bin Wang, International Pacific Research Center, University of Hawaii at Manoa, 1680 East–West Rd., Post Box 401, Honolulu, HI 96822.
E-mail: bwang@soest.hawaii.edu

TABLE 1. Acronym names used in the text, tables, and figures.

(a) Institutions

Acronym	Full names of participating institute
COLA	Center for Ocean–Land–Atmosphere Studies (United States)
DNM	Institute of Numerical Mathematics (Russia)
NASA GSFC	National Aeronautics and Space Administration Goddard Space Flight Center (United States)
GFDL	Geophysical Fluid Dynamics Laboratory (United States)
IAP	Institute of Atmospheric Physics (China)
IITM	Indian Institute of Tropical Meteorology (India)
MRI	Meteorological Research Institute (Japan)
NCAR	National Center for Atmospheric Research (United States)
NCEP	National Centers for Environmental Prediction (United States)
SNU	Seoul National University (Korea)
SUNY	State University of New York (United States)

(b) Other

Acronym	Expansion
A-AM	Asian–Australian monsoon
AGCM	Atmospheric general circulation model
AMIP	Atmospheric Model Intercomparison Project
AUSMI	Australian monsoon index
CLIVAR	International Research Program on Climate Variability and Predictability
CMAP	Climate Prediction Center Merged Analysis of Precipitation
ENSO	El Niño–Southern Oscillation
GEOS	NASA GSFC Earth Observing System
GISST	Global Sea Ice and Sea Surface Temperature dataset
IMI	Indian monsoon index
ISM	Indian summer monsoon
ReA	NCEP–NCAR reanalysis data
SIO	Southern Indian Ocean
WNP	Western North Pacific
WNPMI	WNP monsoon index
WYI	Webster–Yang index

been attributed to the models' superior simulations of climatology. For instance, Sperber and Palmer (1996) found that better simulation of interannual variation in Indian rainfall is associated with better simulation of the mean rainfall climatology. Gadgil and Sajani (1998) noticed that the models with realistic simulations of the primary rainbelt's seasonal migration over the Asian–Pacific sector have much higher skill in simulating Indian summer rainfall than those models in which the seasonal migration is small. On the other hand, Soman and Slingo (1997) hypothesized that realistic simulation of the rainfall variability in the western Pacific may be a key to the realistic simulation of a strong or weak Indian summer monsoon rainfall in turn associated with ENSO. Liang et al. (2001) discussed biases in AMIP model simulations of the east China summer monsoon and Zhang et al. (1997) assessed the simulations of the winter monsoon. Unfortunately, little attention has been paid to assessing the models' performance in simulating the variability of the western North Pacific summer monsoon.

AMIP covered the period 1979–88 in which only two ENSO cycles occurred. The models were able to simulate the all-Indian monsoon rainfall well during the 1987–88 El Niño–La Niña events, but not during the 1982–83 events. It is unclear what caused this inconsistency. Needed is an analysis of the performance of the models over a period that includes more ENSO cycles. This study examines the A–AM variability over a 49-yr period in ensemble simulations with the Seoul National University AGCM.

The unprecedented strength of the 1997/98 El Niño had a phenomenal influence on global climate. It developed dramatically in summer 1997, reached a record peak in December 1997 with the Niño-3.4 (5°S–5°N, 170°–120°W) SST anomaly exceeding 3.0°C, and then decayed rapidly into a La Niña phase during June–August of 1998 (McPhaden 1999). Note, however, that the all-Indian rainfall during 1997 was nearly normal. This is at odds with the negative correlation between ENSO and Indian rainfall that was derived from a long-term dataset (e.g., Angell 1981; Rasmusson and Carpenter 1983, and many others). These peculiar aspects make the exceptionally strong 1997/98 El Niño a unique case for assessing the capability of the current AGCMs in simulating the A–AM anomalies.

Recently, the Climate Variability and Predictability (CLIVAR)/International Monsoon Panel initiated a monsoon AGCM intercomparison project focusing on ENSO and the monsoon anomalies associated with the 1997/98 El Niño (Kang et al. 2002a; all acronym names are defined in Table 1). Several aspects were examined, including the climatological annual variations in the Asian summer monsoon (Kang et al. 2002b), the ENSO-

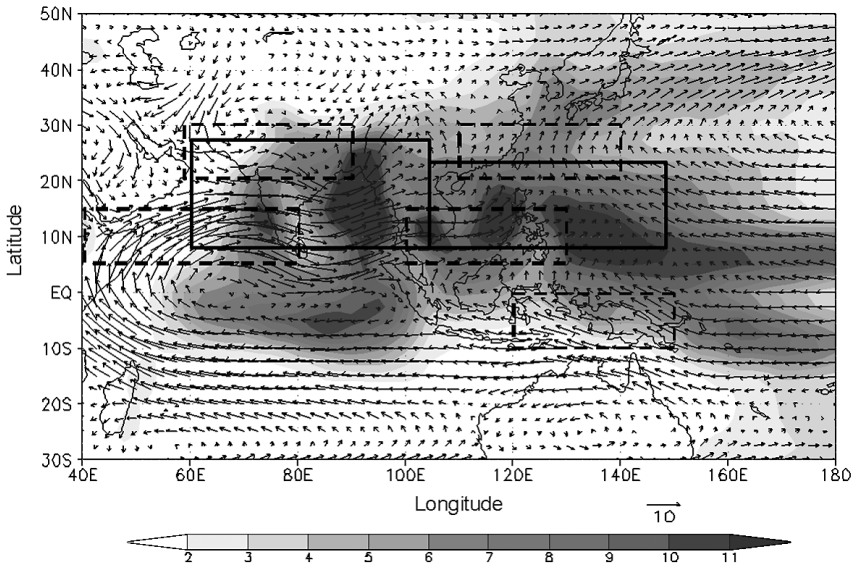

FIG. 1. Jun–Sep mean 850-hPa winds (arrows) and CMAP (Xie and Arkin 1997) precipitation rate (gray shading in units of mm day^{-1}). The two solid-line boxes indicate the locations of the precipitation indices defined for the Indian region and WNP, respectively. The dashed-line boxes indicate locations in which the Indian, NWP, and the Australian monsoon indices are defined (see text for details).

induced anomalies (Kang et al. 2002a), and the intraseasonal variability of the monsoon (Wu et al. 2002; Waliser et al. 2002). Kang et al. (2002a) found that most models capture the rainfall anomalies in the tropical central-eastern Pacific well, but have difficulty in simulating anomalies over the Maritime Continent. Their study primarily focuses on the tropical rainfall anomalies over the entire ENSO and the monsoon regions (40°E–70°W) and on the upper-level winter circulation anomalies in the Pacific–North American region. The present study complements the analysis of Kang et al. (2002a), focusing on variability in the A–AM system during the 1997/98 El Niño, in particular the evolution of A–AM anomalies from its development to decay phase (section 3).

Instead of focusing on the local Indian summer rainfall, this study examines large-scale monsoon rainfall anomaly patterns. The A–AM covers more than one-third of the global Tropics from roughly 40° to 160°E (Fig. 1) and exhibits huge regional variability in climatology (Wang and LinHo 2002) as well as interannual variability, with the largest differences occurring between the Indian and western North Pacific (WNP) summer monsoons (Tao and Chen 1987; Wang et al. 2001). The local air–sea interaction plays different roles in modulating ENSO's impacts on the Indian monsoon (Lau and Nath 2000) and the western North Pacific (Wang et al. 2000). Therefore, this study pays special attention to the differences in simulating the anomalous Indian, WNP–East Asian, and Australian monsoon subsystems (section 4).

The main goal of this study is to identify systematic errors that are common to the 11 AGCMs under examination. Section 5 shows that the poor simulation in summer rainfall is a common characteristic of all the models and is due mainly to a lack of skill over Southeast Asia and the western North Pacific. It is further revealed that the models' deficiencies result from a failure to simulate correctly the relationship between the local rainfall and SST anomalies over the Philippine Sea, the South China Sea, and the Bay of Bengal. The reasons for the models' common problem are discussed in the last section, in which concluding remarks are presented.

2. The experimental framework and evaluation methods

a. The AGCM Intercomparison Project and the data

Kang et al. (2002b) presented an overview of the CLIVAR/A–AM Panel AGCM Intercomparison Project, which follows the same design as AMIP (Gates et al. 1999). The eleven AGCM groups that participated in this project are listed in Table 1. For a detailed description of the AGCMs and their experimental designs, readers are referred to Table 1 of Kang et al. (2002a).

Each participant performed a suite of 10 ensemble runs with different initial conditions for the 2-yr period from 1 September 1996 to 31 August 1998 using an identical SST as the lower boundary forcing. The SST data prescribed in the AGCM experiments are observed pentad means from the Global Sea Ice and Sea Surface Temperature dataset (GISST; Rayner et al. 1996). The

sea ice was specified using climatological monthly mean data adopted by AMIP. For simplicity, we refer to the results obtained from the 10 ensemble experiments of each model as the model ensemble means. The results obtained by averaging all 11 participating models (ensemble means) are referred to as model composites.

The data used to validate the models are from the NCEP–NCAR reanalysis dataset (Kalnay et al. 1996, hereafter reanalysis), and the Climate Prediction Center Merged Analysis of Precipitation (CMAP; Xie and Arkin 1997). This dataset utilizes infrared and microwave satellite data and in situ observations to estimate pentad mean precipitation averaged over an area of $2.5° \times 2.5°$ latitude–longitude. The accuracy of the precipitation data over the oceans is difficult to establish due to a lack of ground truth observations. Significant differences were found over the western Pacific compared to other estimated precipitation values, such as the Global Precipitation Climatology Project precipitation (Gruber et al. 2000). Nevertheless, it is more reliable than reanalysis precipitation and we believe it provides a reasonable reference for model validation for monthly mean anomalies.

b. Assessment methods

Our evaluation of the models' performances emphasizes their ENSO-phase-dependent evolution and characteristics (presented in section 3). This is because the A–AM anomalies vary with the phase of El Niño; distinguishing between the development- and the decay-phase anomalies over East Asia and WNP during the summer monsoon is essential.

The models' performances in simulating rainfall distributions are evaluated by computing pattern correlation coefficients between the observed and model-simulated rainfall anomaly fields. The pattern correlation coefficients measure the simultaneous spatial correlation between the observed and corresponding simulated fields with the sample size that is determined by the total number of grids.

There are large regional differences in the rainfall and circulation anomalies in the A–AM domain, which covers one-third of the global Tropics (Wang et al. 2001). To facilitate assessing the models' performance on regional monsoon variability, several regional monsoon rainfall and low-level circulation indices are used.

c. Regional monsoon indices

Precipitation indices are defined for the Indian and the WNP monsoon region, respectively. The all-Indian rainfall is often used as a quantity to measure the degree of a model's success in simulating Asian summer monsoon (e.g., Parthasarathy et al. 1992). While this index provides a convenient and most reliable area-averaged rainfall time series, the satellite observations have indicated that the heaviest precipitation in the Asian summer monsoon is located over the Bay of Bengal and in the vicinity of the Philippines. Given the large regional variability of precipitation and the low resolutions of the AGCMs, it is more meaningful to look at the models' precipitation values averaged over two large areas around the heaviest rainfall centers as shown by the solid-line boxes in Fig. 1. The corresponding rainfall rates are referred to as the Indian and WNP monsoon precipitation indices, respectively. The simulated annual cycles for the two indices are compared with observations (Fig. 2). Note the systematic positive bias in the Indian summer monsoon region from May to September (Fig. 2a). In the western North Pacific region from June to October, the model-simulated precipitation not only shows large spreading among individual models, but also exhibits two types of model behavior: one tends to overestimate while the other tends to underestimate the precipitation (Fig. 2b). The spreading among models over the WNP is nearly triple that over the Indian monsoon region. Therefore, the majority of the 11 AGCMs exhibit greater difficulties in reproducing the correct climatology over the WNP than over the Indian monsoon region. Given the fact that the total rainfall over the WNP monsoon region exceeds that over the Indian monsoon region (Fig. 2), this deficiency is a major caveat of the existing AGCMs. Unfortunately, the flaw has not received sufficient attention in the modeling community.

Dynamic monsoon indices are defined for regional monsoon subsystems. Webster and Yang (1992) used the vertical zonal wind shear between 200 and 850 hPa ($U_{200} - U_{850}$) averaged over the South Asian region (0°–20°N, 40°–110°E) to measure the broadscale South Asian monsoon circulation anomalies. This is referred to as the Webster–Yang index (WYI). The variability of the vertical shear is associated with the variability of two convective heat sources: one lies in the Bay of Bengal and the other in the vicinity of the Philippines. The interannual variations of the two convective heat sources, however, are not significantly correlated (Wang and Fan 1999). It is, therefore, imperative to examine the variability of the Indian summer monsoon and western North Pacific–East Asia summer monsoon separately.

To quantify the variability of the Indian and the WNP summer monsoon separately, the meridional differences of the 850-hPa zonal winds (U_{850}) are used to define two circulation indices (Wang and Fan 1999; Wang et al. 2001); that is,

$$\begin{aligned} \text{IMI} &= U_{850}(5°\text{–}15°\text{N}, 40°\text{–}80°\text{E}) \\ &\quad - U_{850}(20°\text{–}30°\text{N}, 60°\text{–}90°\text{E}), \quad \text{and} \\ \text{WNPMI} &= U_{850}(5°\text{–}15°\text{N}, 100°\text{–}130°\text{E}) \\ &\quad - U_{850}(20°\text{–}30°\text{N}, 110°\text{–}140°\text{E}), \end{aligned}$$

where the areas in parentheses denote the regions over which U_{850} is averaged. We note that the IMI (WNPMI)

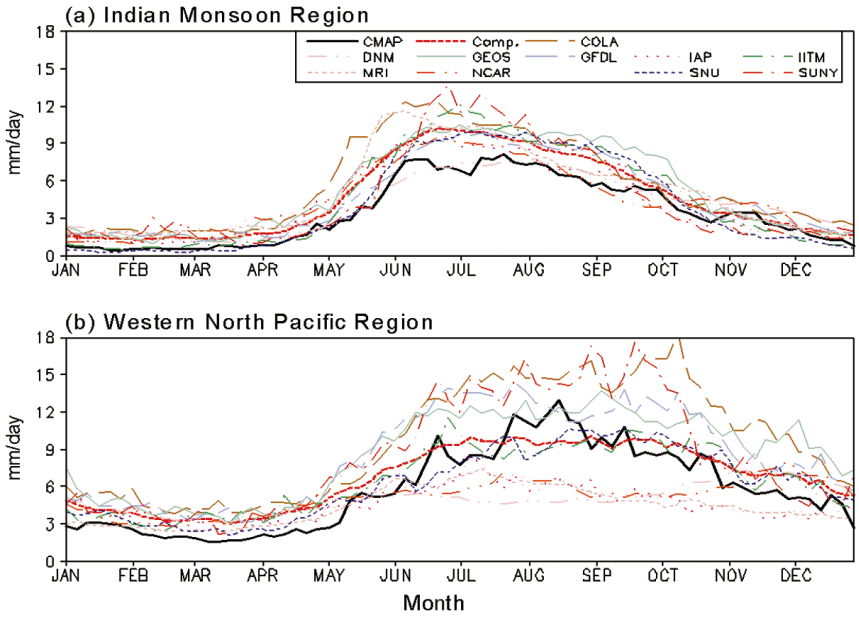

FIG. 2. Climatological pentad mean precipitation anomalies derived from CMAP and from each individual model and the all-model ensemble mean (Comp) for the period 1979–98.

essentially depicts the vorticity of the Indian (WNP) monsoon trough and associated southwesterly monsoon. The IMI is not only highly correlated with the all-Indian rainfall index, with a correlation coefficient of 0.72 for the 50-yr period from 1949 to 1998, but it also is highly correlated with the first EOF mode of the 850-hPa circulation anomalies over the Indian monsoon region (0°–30°N, 30°–100°E) with a correlation coefficient 0.72 for the period 1949–98 (Wang et al. 2001). Similarly, the WNPMI is highly correlated with the dominant EOF mode of 850-hPa winds over the WNP and East Asian summer monsoon domain (0°–40°N, 100°–170°E) with a correlation coefficient 0.88 for the period 1949–98 (Wang et al. 2001). These facts add confidence to the two regional dynamic monsoon indices defined here in terms of their representing the regional monsoon variability.

The Australian summer monsoon is characterized by the presence of equatorial westerlies at 850 hPa overlaid by equatorial easterlies at 200 hPa (Webster 1983; McBride 1987). Following this traditional concept and focusing on low-level monsoon flows, a circulation index is proposed to measure the Australian summer monsoon variability, which is defined by the 850-hPa zonal wind anomalies averaged over 0°–10°S, 120°–150°E. This index is referred to as the Australian monsoon index (AUSMI).

IMI, WNPMI, and AUSMI provide succinct descriptions of the three major subsystems of the A–AM, while WYI measures the broadscale South Asian monsoon. Although these indices were originally designed to quantify the local summer monsoon variability, they are also meaningful indicators for the corresponding winter monsoon anomalies, because the monsoon is characterized by an annual reversal of the low-level winds between summer and winter.

3. Simulated evolution of the monsoon variability during the 1997/98 El Niño

Figure 3 shows observed anomalous 850-hPa winds and precipitation for the consecutive six seasons from spring [March–April–May (MAM)] 1997 to summer [June–July–August (JJA)] of 1998. Figure 4 shows the counterparts derived from the all-model composite.

During the developing phase of the El Niño from MAM to September–October–November (SON) of 1997, prominent features over the Indian Ocean are the rapid development of the equatorial easterly anomalies, the associated southern Indian Ocean (SIO) anomalous anticyclone, and the accompaning suppressed convection in the eastern Indian Ocean and enhanced convection in the western Indian Ocean (Figs. 3a–c). The simulated circulation anomalies are considerably weaker than observed and predominantly confined to the equatorial regions (Figs. 4a–c). During SON 1997, the model-simulated precipitation anomalies exhibit a striking north–south contrast between the equatorial suppressed convection and the South Asian enhanced convection, while the observed precipitation shows a zonal dipole pattern.

Over the Philippine Sea, the low-level circulation changes drastically from JJA 1997 (cyclonic) to SON 1997 (anticyclonic) (Figs. 3b,c). This change was simulated reasonably well in the model composite (Figs. 4b,c). However, in JJA 1997 the pronounced Philippine

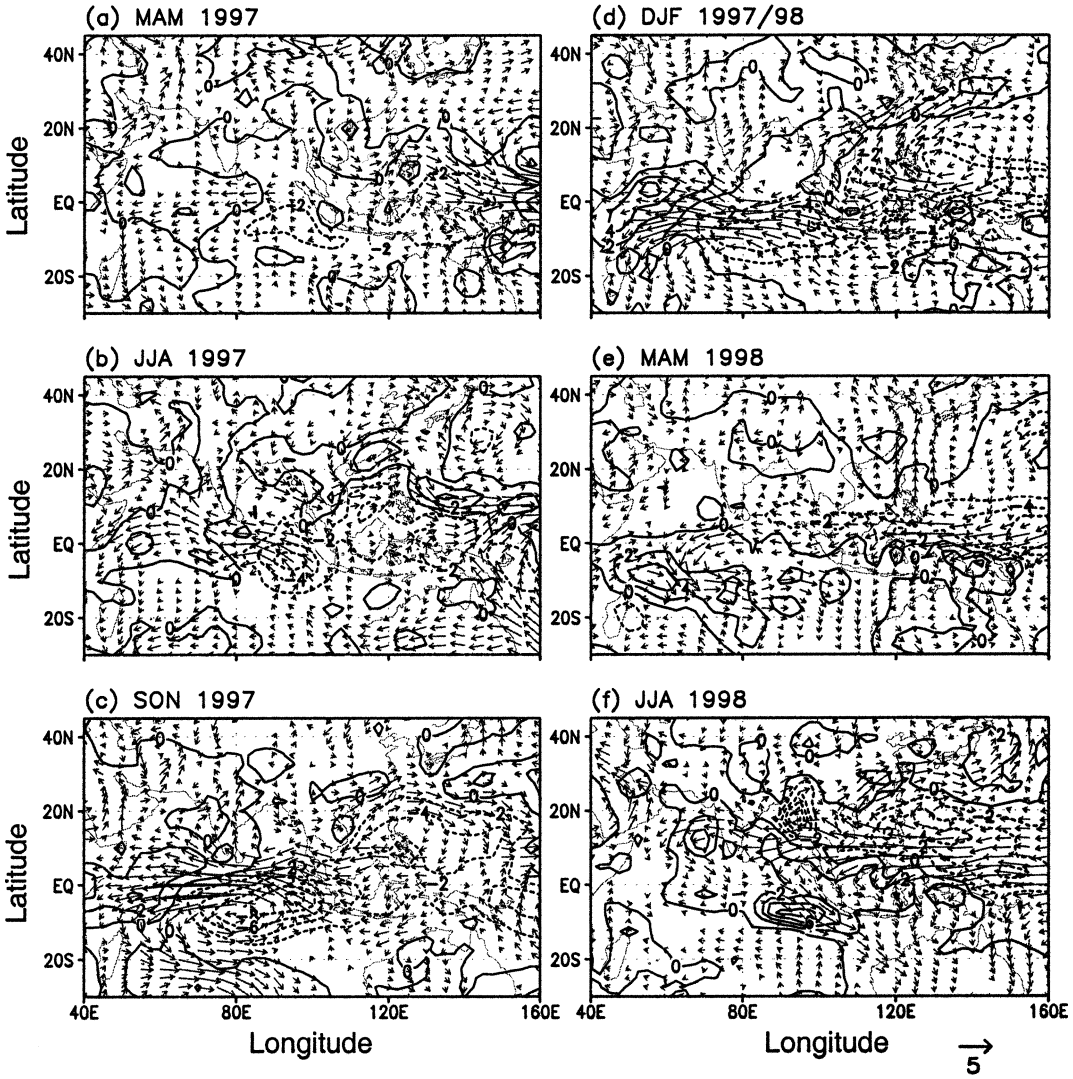

FIG. 3. Observed A–AM anomalies during the 1997/98 El Niño event for six consecutive seasons. Arrows denote 850-hPa anomalous winds (scale is indicated at the bottom in units of m s^{-1}) obtained from the NCEP–NCAR reanalysis (Kalney et al. 1996). Solid (dashed) contours represent a positive (negative) anomalous precipitation rate (mm day^{-1}) derived from CMAP (Xie and Arkin 1997).

Sea–Japan dipole circulation pattern is totally missed in the model composite, hinting at a serious limitation in the models' response to ENSO forcing in the extratropical region.

During the mature phase of the El Niño (DJF1997/98), the observed low-level circulation anomalies are dominated by two anticyclonic anomalies located over the WNP and SIO, respectively (Fig. 3d). These circulation anomalies are well captured in the model composite (Fig. 4d) as well as by individual model ensemble simulations (figure not shown). The precipitation anomalies in the A–AM region during DJF1997/98 are also reproduced reasonably well.

During the decay phase (MAM 1998 and JJA 1998), the pronounced WNP anticyclone maintains itself; the associated easterly anomalies penetrate from WNP into the South Asia (Figs. 3e,f). The model composite captures these features realistically (Figs. 4e,f). However, the rainfall anomalies in JJA 1998 have large discrepancies in the Southeast Asia region, including the area from the Bay of Bengal to the Philippine Islands.

In summary, the boreal winter and spring A–AM anomalies (both circulation and precipitation) are much better simulated than those during the boreal summer and fall. The low-level circulation anomalies over the western Pacific sector (the WNP anticyclone) are better captured than those in the Indian sector (the SIO anticyclone). The precipitation anomalies and the Indian Ocean circulation anomalies in the model composite are weak mainly due to large spreading among individual

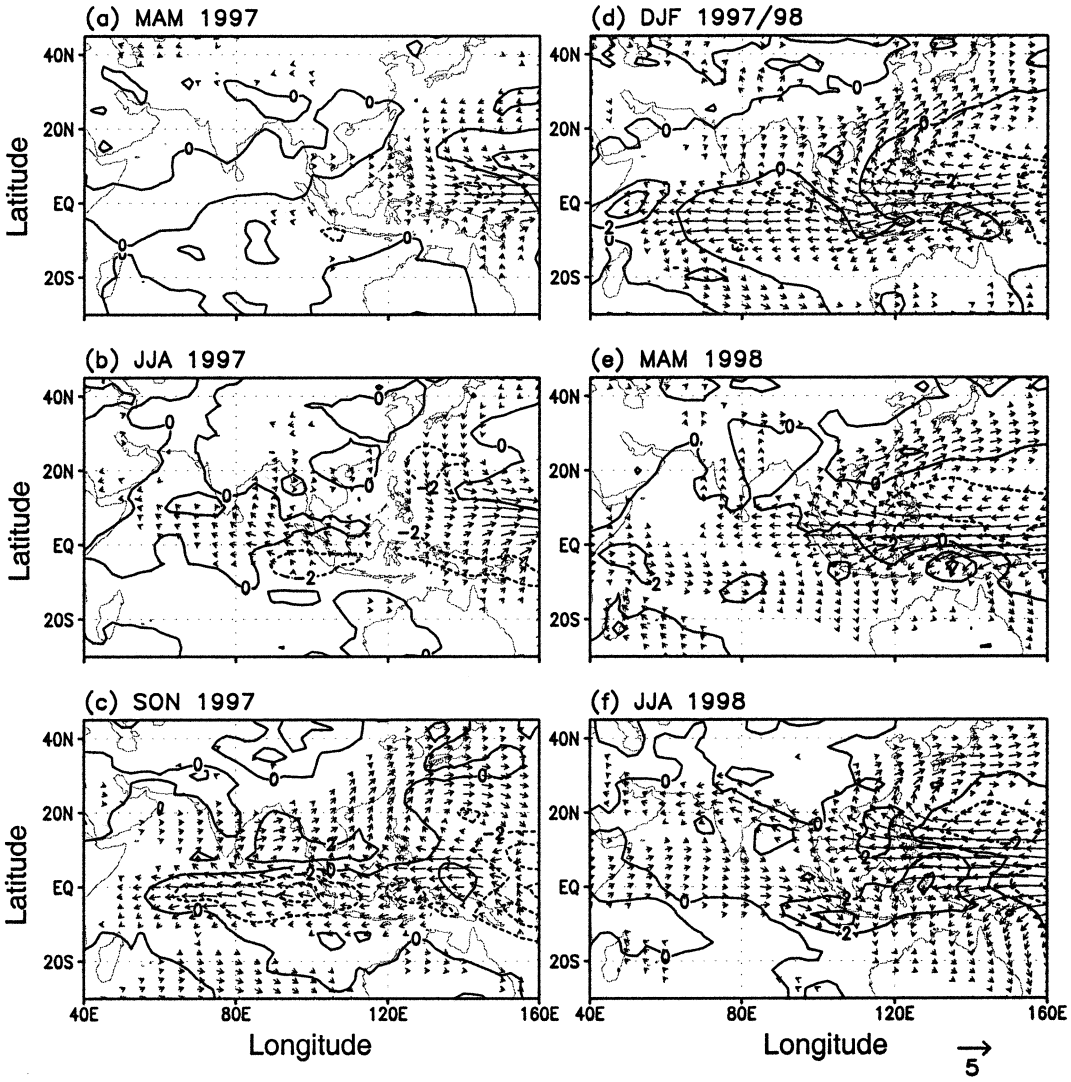

FIG. 4. Same as in Fig. 3 except for the all-model composite.

model simulations. Precipitation anomalies during boreal summer and fall are most problematic in the model simulation.

4. Regional differences in simulation of rainfall and circulation anomalies

a. Comparison of the A–AM and El Niño regions

Kang et al. (2002a) have assessed the 11 models' simulations of rainfall anomalies over the entire tropical Pacific and Indian Ocean region. To compare the difference between the simulations of the A–AM and El Niño regions, we divide the ENSO–monsoon domain (30°S–30°N, 40°E–80°W) into two sectors: the A–AM region (30°S–30°N, 40°–160°E) and the El Niño region (30°S–30°N, 160°E–80°W), each covering one-third of the global Tropics. The pattern correlation coefficients between observed and simulated precipitation anomalies (Fig. 5) are used to score the model's skill.

In the El Niño region, all models simulate realistic rainfall anomalies; the correlation coefficients between the observed and simulated patterns range from 0.6 to 0.9 in individual models and exceed 0.85 for the model composite (Fig. 5a). Even when SST anomalies are moderate in DJF1996/97, the pattern correlation for precipitation in the El Niño region remains significant (about 0.6). These results point to a sensitive dependence of precipitation anomalies on local SST anomalies in the eastern-central Pacific. Nearly all models reproduce the rainfall anomaly patterns reasonably well as long as the SST anomaly reaches moderate strength, such as in the DJF1996/97.

In sharp contrast, the pattern correlations in the A–AM region are substantially poorer in both the individual model ensemble means and the model composite

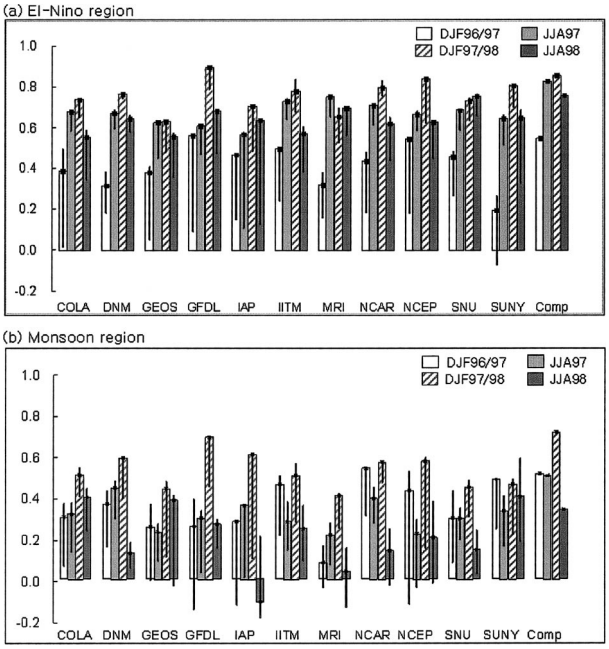

FIG. 5. Pattern correlation coefficients between observed and simulated precipitation anomalies over (a) the El Niño region (30°S–30°N, 160°E–80°W) and (b) the A–AM region (30°S–30°N, 40°–160°E). The coefficients were computed for each model's ensemble experiments and from the all-model ensemble mean (Comp). The line segments in the bar diagrams denote the ranges of correlation coefficients of individual experiments. The filled squares denote the individual model ensemble means.

(Fig. 5b). In addition, the composite pattern correlation coefficients during the peak phase of ENSO (DJF1997/98) range from 0.4 to 0.7. This is considerably higher than those during JJA1997, for which the pattern correlation coefficients vary from 0.22 to 0.45 with the model composite about 0.54—a value that is even lower than that in DJF1996/97 when SST anomalies are rather weak. Obviously, the precipitation anomalies over the A–AM domain respond more robustly to anomalous SST forcing during boreal winter than summer. This assertion is consistent with that derived from comparison of Figs. 3 and 4. The sharp decrease in model performance during boreal summer indicates that the strong 1997/98 El Niño forcing does not control the Asian summer monsoon rainfall anomalies.

During boreal winter the pattern correlation between the observation and the model composite is comparable or even worse than the pattern correlations derived from some individual models such as GFDL, NCAR, NCEP, and SUNY (Fig. 5a). On the other hand, in the A–AM region, the pattern correlation of the model composite tends to be significantly higher than that derived from each individual model (Fig. 5b). This is likely due to the fact that the boreal summer monsoon rainfalls produced by different models are more independent of each other. Their composite therefore attains a significantly higher pattern correlation coefficient. When individual models have relative high skills, the simple composite may not result in a better result. In that case, the superensemble technique (Krishnamurti et al. 2000), which assigns each model a different weight in the same region, should be used for multimodel ensemble climate prediction.

b. Comparison of regional monsoon circulation anomalies

Figure 6 compares time series of the four monsoon circulation indices defined in section 2 for the entire South Asian monsoon (WYI), as well as the Indian, WNP, and Australian monsoon subsystems. First, the seasonal dependence of the models' skills is obvious: during the local summer season (June–October for Indian and WNP and December–March for Australian monsoons). The spreading among the models is considerably larger during the summer season than that during local winter for all indices. Second, nearly all models simulate realistic WNP and Australian monsoons (Figs. 6c,d) but simulate very poor Indian monsoon circulation anomalies (Fig. 6b) throughout the 2-yr period. The monthly correlation coefficient for the model composite reaches 0.65 for both Australian and WNP monsoons with a sample size of 264 (Table 2). In contrast, the Indian monsoon circulation index (computed for the model ensemble) is not significantly correlated with the observed counterpart (Table 2). For the broadscale South Asian monsoon circulation, the models' performance in terms of WYI is in between those of WNPMI and IMI (Fig. 6a; Table 2).

The results here show remarkable regional differences in the performance of the AGCM simulations of the variable A–AM system. The current AGCMs reproduce monsoon circulation variability over the Australian and western Pacific–East Asian monsoon regions, but have fundamental difficulties in simulating the Indian monsoon circulation variability. The Indian monsoon circulation index is defined for a much larger region over India and the northern Indian Ocean. The failure is not due to an absence of Indian monsoon circulation anomalies (Fig. 6c), but due to model deficiencies.

Because the above statement is based on a short 2-yr integration covering only the 1997/98 El Niño, it is necessary to verify it against long-term integrations. For this purpose, the SNU model was used to perform a suite of five AMIP-type runs for January 1950–December 1998. The results are shown in Fig. 7. The model ensemble mean is generally better correlated with the reanalysis than the individual experiment is correlated with the four circulation indices.

There are notable differences between the long-term integration (Fig. 7) and the 2-yr integration. For convenience we compare the seasonal mean anomalies. In the 2-yr integration of the SNU model the seasonal correlation coefficients for WYI (-0.20) and IMI (-0.13) are completely different from those in the long-term

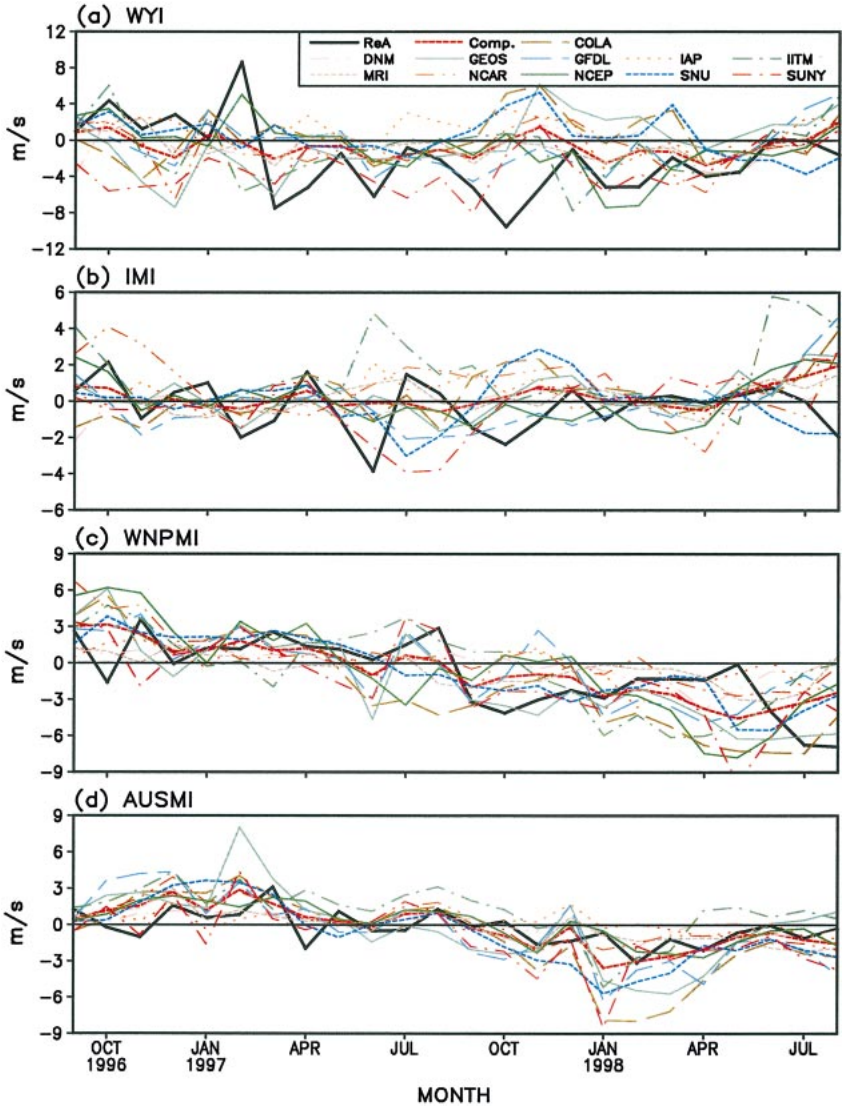

FIG. 6. Time series of monthly mean anomalous monsoon circulation indices: (a) WYI, (b) IMI, (c) WNPMI, and (d) AUSMI. These indices are derived, respectively, from the NCEP–NCAR reanalysis (ReA), the all-model ensemble mean (Comp), and from each model's 10-member ensemble mean for the period Sep 1997–Aug 1998. The monsoon circulation indices are defined in section 2. The acronyms for the AGCMs are explained in Table 1.

runs for WYI (0.50) and IMI (0.30) (Figs. 7a,b). This indicates that the models' performance in simulating monsoon anomalies associated with the strong 1997/98 El Niño indeed differs quantitatively from those associated with all ENSO events during the 1950–98 period. During 1997/98 El Niño, the models experienced unusual difficulty in reproducing correct Indian summer monsoon anomalies and the broadscale South Asian

TABLE 2. Correlation coefficients between the NCEP–NCAR reanalysis and the model ensemble means (for each individual model and the all-model composite). Computations were carried out for four monsoon indices and using monthly mean data. The acronym expansions are provided in Table 1.

	Comp	COLA	DNM	GEOS	GFDL	IAP	IITM	MRI	NCAR	NCEP	SNU	SUNY
AUSMI	0.65	0.63	0.57	0.55	0.41	0.29	0.44	0.51	0.60	0.60	0.64	0.43
IMI	0.08	−0.21	−0.19	0.06	−0.11	−0.46	−0.04	−0.11	0.04	0.23	−0.12	0.06
WNPMI	0.65	0.54	0.32	0.68	0.49	0.50	0.34	0.39	0.51	0.41	0.65	0.51
WYI	0.34	−0.35	0.11	−0.16	0.33	0.11	0.05	0.33	−0.02	0.53	−0.20	−0.05

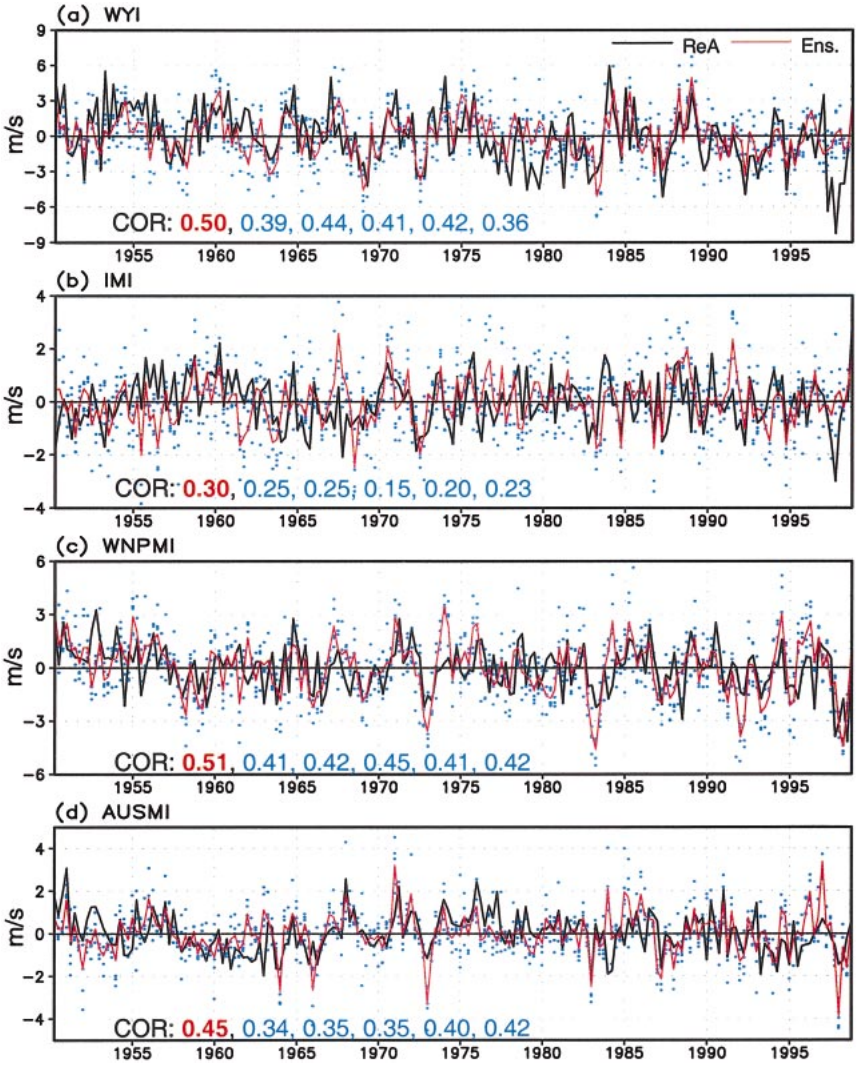

FIG. 7. Time series of seasonal mean anomalous monsoon circulation indices for the period 1950–98 derived from ReA and from the five-member ensemble mean (Ens) as well as each experiment (dots) using the SNU model. The numbers listed in each panel (R) denote the correlation coefficients between ReA and Ens (red) and between the ReA and each experiment (blue).

monsoon circulation. This can be seen clearly from Figs. 7a,b.

Figure 8 reveals that observed WYI has a linear decreasing trend during the last 50 yr, suggesting the broadscale South Asian monsoon circulation has been weakening. However, the model composite did not show this trend.

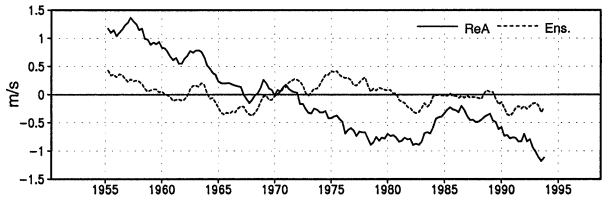

FIG. 8. Ten-year running mean time series of the WYI derived from ReA and the five-member ensemble mean (Ens) in the SNU model simulation.

c. Comparison of the Indian and WNP monsoon precipitation anomalies

Figure 9 shows time series of monthly mean precipitation rates averaged over four large monsoon regions: (a) the WNP monsoon region (7.5°–22.5°N, 105°–150°E), (b) the Indian summer monsoon (ISM) region (7.5°–27.5°N, 60°–105°E), (c) the East Asian subtropical monsoon region (22.5°–45°N, 105°–140°E), and (d) the maritime continental region (10°S–5°N, 90°–150°E). Over these monsoon regions, the model composites gen-

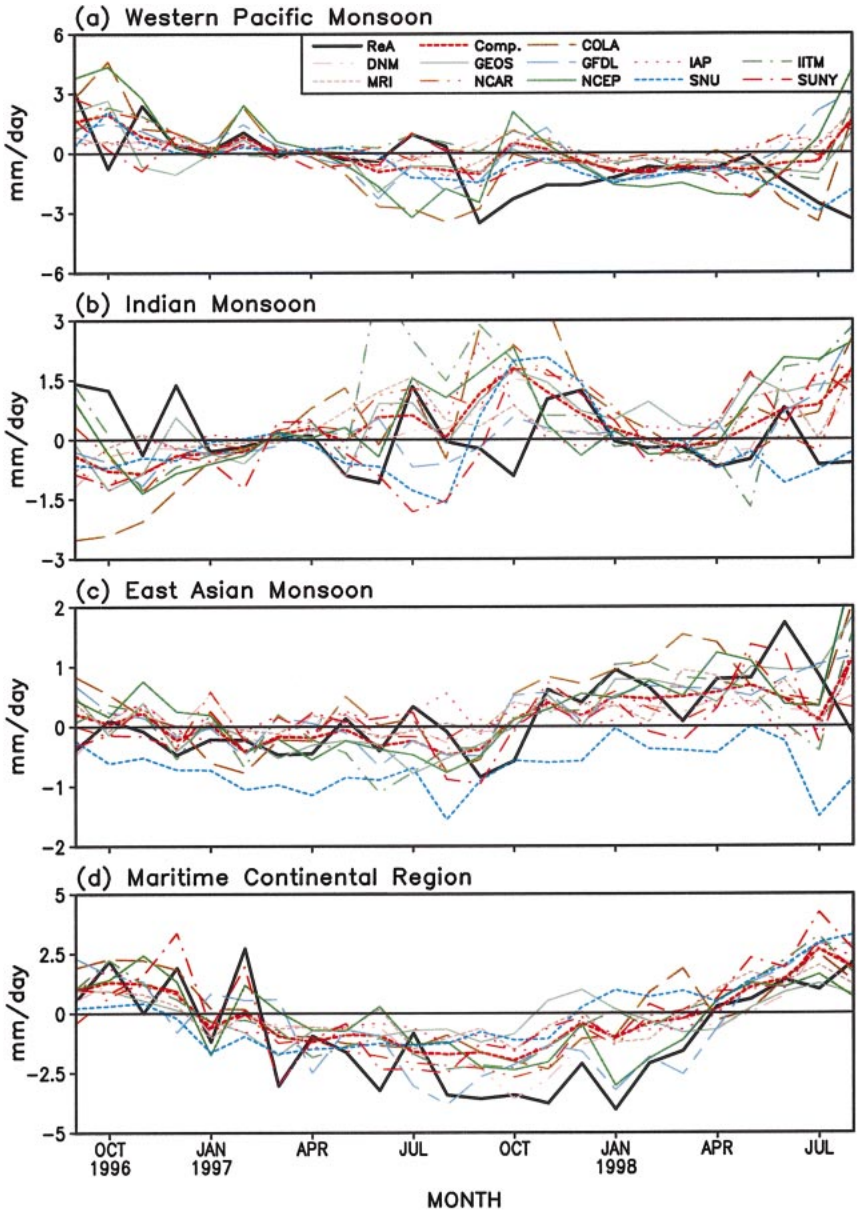

FIG. 9. Time series of the monthly mean precipitation rate anomalies averaged over (a) the WNP monsoon (7.5°–22.5°N, 105°–150°E), (b) the Indian monsoon (7.5°–27.5°N, 60°–105°E), (c) the East Asian monsoon (22.5°–45°N, 105°–140°E), and (d) the Maritime Continental region (10°S–5°N, 90°–150°E).

erally display considerable discrepancies during the local rainy seasons: May–October over the ISM, June–November over the WNP summer monsoon, and June–September over the East Asian summer monsoon regions. However, during the dry season, the model composites resemble CMAP closely, especially from December to April. The model composite captures the rainfall over the Maritime Continent very well qualitatively, but the amplitude is substantially underestimated during the developing and mature phases of the 1997/98 El Niño, that is, JJA1997, SON1997, and DJF1997/98 (Fig. 9d). This reduction of amplitude results in part from large discrepancies in the rainfall patterns among individual model ensemble means, which means that the AGCMs have difficulty in capturing the location of the sinking branch of the anomalous Walker circulation.

5. Why the rainfall anomalies in the A–AM region are poorly simulated

Various hypotheses were tested. For instance, the poor simulation is assumed to be related to (a) a poor sim-

ulation of the climatological mean state in this region, (b) a poor simulation of the precipitation anomalies in the El Niño region (i.e., poor simulation of remote forcing), or (c) a poor simulation of the Maritime Continent sinking branch of the anomalous Walker circulation (which in turn affects the simulated rainfall in the other monsoon regions). Unfortunately, our analyses of the multimodel ensemble means do not support any of the above hypotheses. For brevity, figures are not shown but conclusions are summarized as follows. The model performances in simulating the A–AM rainfall anomaly patterns during boreal summer depend neither on their skill in the simulation of the rainfall climatology nor on their performance in simulating the rainfall anomaly patterns over the El Niño region. Better simulation of anomalous El Niño rainfall patterns does not warrant a better simulation of those over the Maritime Continent, and superior simulations over the Maritime Continent are not indicative of better simulations of anomaly patterns over the rest of the A–AM domain.

Careful scrutiny of the observed and model-simulated rainfall anomaly patterns reveals that the model's performances over the entire A–AM region are not homogeneously poor. Rather, we identify that the performance is extremely unskillful only over a specific subdomain while it is reasonably good over the rest of the A–AM regions. This subdomain in which the models' performances are extremely poor covers Southeast Asia and the WNP region (5°–30°N, 80°–150°E).

Figure 10 compares the observed and model composite precipitation anomalies for JJA1997, SON1997, and JJA1998. Let us focus on the oceanic regions spanning from 5° to 30°N and from 80° to 150°E, which include the Bay of Bengal, the South China Sea, and the tropical western North Pacific (see the boxes in Fig. 10). In these oceanic regions, the all-model composite precipitation anomalies exhibit huge errors. Often the model-simulated and observed rainfall anomalies exhibit opposite signs. For instance, in JJA1997, the observed rainfall over the Philippine Sea is above normal, whereas the model composite yields below normal rainfall in SON1997 and JJA1998. The observed rainfall is below normal over the Bay of Bengal and the South China Sea, yet the all-model composite shows positive precipitation anomalies. Therefore, we identify that the major problem with the rainfall simulation is primarily in the tropical WNP region.

The above finding is further confirmed by the results shown in Fig. 11, in which the pattern correlation coefficients between observed and simulated precipitation anomalies are computed for the following two subdomains: 1) Southeast Asia and the WNP region (5°–30°N, 80°–150°E), that is, the boxed area in Fig. 10, which includes both the ocean and land areas, and 2) the rest of the A–AM domain (30°S–30°N, 40°–160°E, excluding Southeast Asia and the WNP). In Southeast Asia and the WNP region, the pattern correlation coefficients during JJA1997, SON1997, and JJA1998 range from -0.4 to $+0.3$ in individual models and the range is nearly zero for the all-model composite (Fig. 11a). In sharp contrast, in the rest of the A–AM region, the pattern correlation coefficients are substantially higher in both the individual models and the model composite (Fig. 11b). The model composite and observed pattern correlation coefficients reach 0.7. Obviously, the low skill in simulating the Asian summer monsoon rainfall anomalies is primarily caused by the extremely poor simulation in Southeast Asia and the WNP. This is particularly true over the South China Sea and tropical WNP.

To better understand why the models tend to produce erroneous simulations of summer rainfall, we examined the relationship between the local monthly mean SST and rainfall anomalies. The correlation coefficients between the monthly mean anomalies of the local SST and precipitation (at each 2.5° latitude by 2.5° longitude grid) in the oceanic areas of the boxed subdomain (total of 222 grids) were computed. The results are shown in Table 3. For the three seasons (JJA1997, SON1997, and JJA1998) as a whole, the observed monthly mean CMAP rainfall anomalies are *negatively* correlated with local SST anomalies with a correlation coefficient of -0.35 (significant at the 99% confident level with a sample size of $222 \times 9 = 1998$ for the domain), whereas the model composite rainfall anomalies are *positively* correlated with the local SST anomalies with a correlation coefficient of 0.58. In fact, virtually all the individual model ensemble mean anomalies are positively correlated with local SST anomalies; none of them reproduces the observed negative correlation (Table 3). It is concluded that the poor simulation of the rainfall anomalies in Southeast Asia and the WNP is due to the fact that the models failed to produce the correct local anomalous rainfall–SST relationship.

The simulated intensity of the rainfall anomaly in the A–AM region is found to depend on the models' skill in simulating the rainfall anomalies over the El Niño region. The root-mean-square (rms) of the precipitation anomalies simulated by a model (ensemble mean) is normalized by the observed counterpart. This ratio measures the intensity of the simulated rainfall anomalies as compared to the observation. If the normalized rms is less (greater) than 1, the mean intensity of the simulated anomalies is weaker (stronger) than that of the observation. Figure 12 shows the normalized rms of the precipitation anomalies simulated by each model. The simulated rainfall intensity in the A–AM region increases with increasing performance in the simulated intensity of the rainfall anomalies in the El Niño region. Note also that the simulated monsoon rainfall anomalies during northern winter (the Australian summer monsoon) are weaker than their observed counterparts. This is a hint that the model's ensemble means tend to underestimate the effect of the remote forcing on the maritime Continent and Australian summer monsoon rainfall.

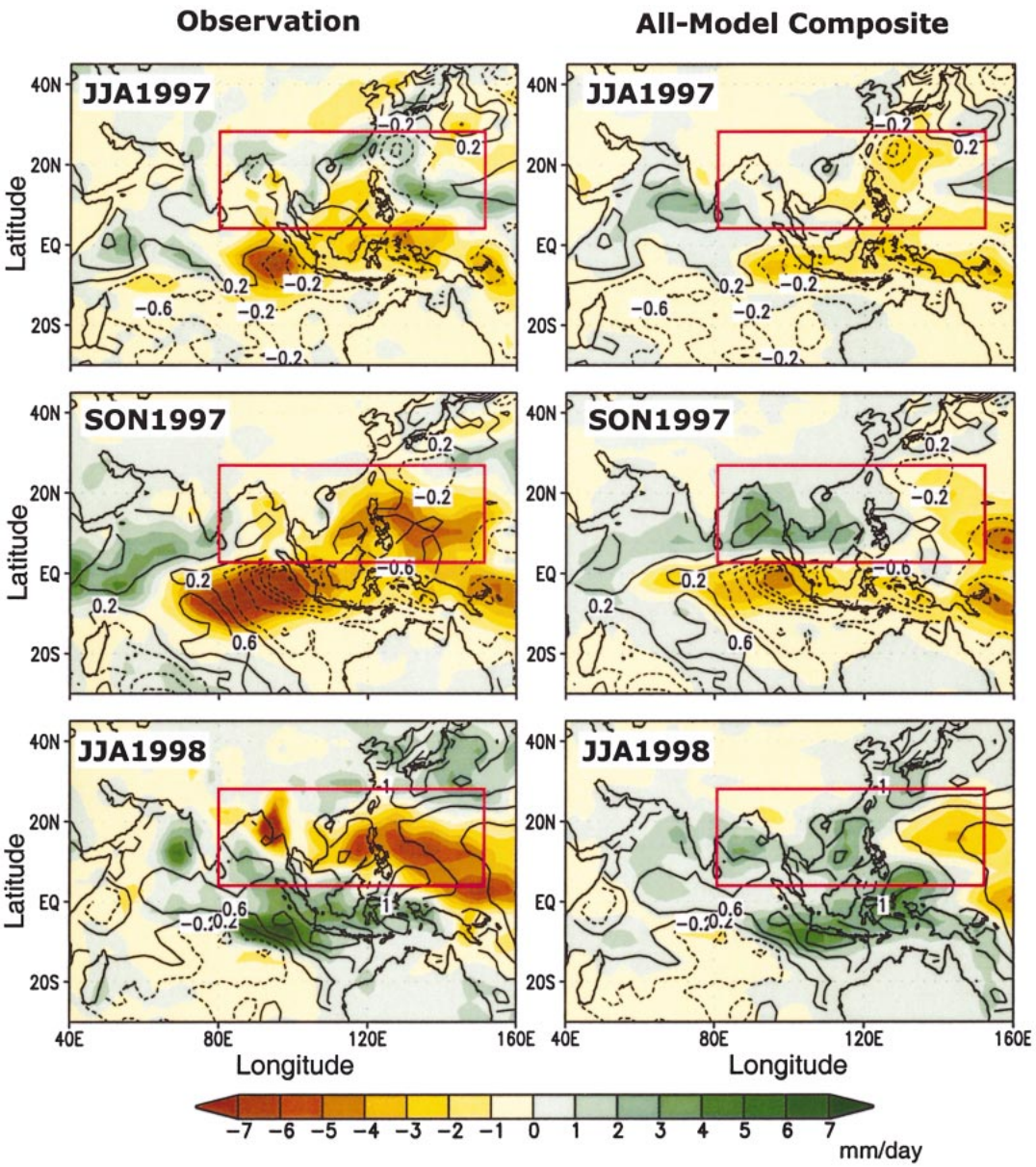

FIG. 10. Precipitation anomalies (color shading) and SST anomalies (contour interval is 0.4 K) for JJA-97, SON-97, and JJA-98. The left (right) three panels are for observations (all-model composite). The redline box outlines Southeast Asia and the tropical western Pacific region, where the models' performance is without skill.

6. Concluding remarks

a. Conclusions

The ability of each of the 11 AGCMs participating in the CLIVAR/A–AM Panel Intercomparison Project (designed to simulate the anomalous monsoon conditions associated with the unprecedented 1997/98 El Niño) was evaluated by 10-member ensemble simulations. They were run from 1 August 1996 to 31 July 1998. The evaluations were focused on precipitation and low-level circulation anomalies. The following aspects were examined: 1) the evolution of the A–AM anomalies from the development to the decay of the 1997/98 El Niño; 2) the quantitative skills in simulating low-level monsoon circulation anomalies, which were measured by evaluating four dynamic monsoon indices representing the broadscale South Asian monsoon, the Indian monsoon, the western North Pacific monsoon, and the Australian monsoon, respectively; and 3) the quantitative skills in simulating the rainfall anomalies in terms of their ability to reproduce the overall pattern correlation and the precipitation indices averaged around two major rainfall centers over the Indian and WNP summer monsoon regions.

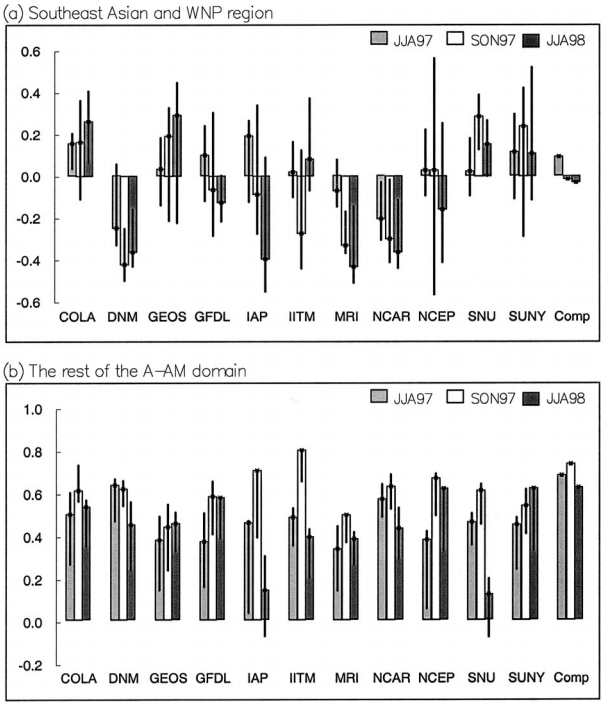

FIG. 11. As in Fig. 5 except for (a) Southeast Asia and the tropical WNP region (the regions spanning from 5° to 30°N and from 80° to 150°E) and (b) the rest of the A–AM domain (30°S–30°N, 40°–160°E) and for JJA1997, SON1997, and JJA1998.

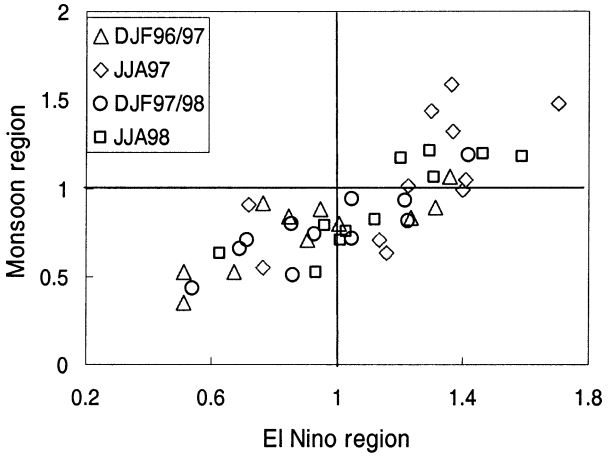

FIG. 12. Scatter diagram showing the positive correlation in the observed–simulated amplitude of the anomalies (as measured by the normalized rms) between the rainfall anomalies over the El Niño region (abscissa) vs those over the A–AM region (ordinate).

Major conclusions are summarized as follows:

1) Most of the 11 models reproduced the low-level circulation anomalies and the variability of the dynamic monsoon indices over the Australian and western North Pacific monsoon regions realistically. They, however, failed with the Indian monsoon (Figs. 3, 4, and 6c,d). To see whether this is generally the case, a suite of five Seoul National University model runs with the same observed lower boundary forcing (differing only in their initial conditions) were examined for the period 1950–98. The skill of this 49-yr ensemble simulation of the Indian monsoon is significantly higher than the skill of the same model for the period of 1996–98. This suggests that for the unprecedented strong 1997/98 El Niño episode, the models under study experience unusual difficulties in simulating the Indian monsoon circulation anomalies (Fig. 7b) and the broadscale Asian summer monsoon as measured by the Webster–Yang index (WYI). In addition, the observed WYI shows a linearly decreasing trend over the last 50 yr, suggesting the broadscale South Asian monsoon circulation has been weakening. However, the model composite of five runs failed to show this trend.
2) The model's performance in simulating boreal summer rainfall anomaly patterns in the A–AM region (30°S–30°N, 40°E–160°E) is generally poor, especially when compared with their performance over the El Niño region (30°S–30°N, 160°E–80°W) (Fig. 5). It is found that the simulated *strength* of the A–AM rainfall anomalies increases with increasing intensity of the rainfall anomaly in the El Niño region. However, the models' skill in simulating Asian summer monsoon rainfall anomaly *patterns* depends neither on their performance in simulating anomalous rainfall patterns over the El Niño region nor on their skill in simulating rainfall climatology. Furthermore, better simulations over the Maritime Continent are not indicative of superior simulations of anomaly patterns over the rest of the A–AM domain.
3) The poor simulation of the boreal summer rainfall anomalies is due mainly to a lack of skill over the subregion 5°–30°N, 80°–150°E. In the rest of the A–AM regions, the rainfall pattern correlation coefficient is reasonably high (around 0.7) for JJA-

TABLE 3. Correlation coefficients between the local SST and precipitation anomalies that are observed (CMAP) or derived from the all-model composite (Comp) and from each model's ensemble means. Acronym expansions are provided in Table 1. Computations were carried out for JJA1997, SON1997, and JJA1998, and the three seasons as a whole using monthly mean data.

	CMAP	Comp	COLA	DNM	GEOS	GFDL	IAP	IITM	MRI	NCAR	NCEP	SNU	SUNY
JJA1997	−0.15	0.59	0.42	0.49	0.38	0.19	0.02	0.15	0.49	0.43	0.39	0.36	0.33
SON1997	−0.33	0.71	0.59	0.7	0.5	0.35	0.45	0.49	0.44	0.66	0.37	0.34	0.37
JJA1998	−0.45	0.56	0.19	0.77	0.24	0.52	0.59	0.44	0.5	0.51	0.57	−0.12	0.38
Total	−0.35	0.58	0.33	0.65	0.32	0.42	0.42	0.37	0.47	0.51	0.47	0.04	0.35

SON1997 and JJA1998 (Fig. 12). The poor simulation of the rainfall variability in the above subregion (Southeast Asia and WNP) is a striking characteristic of all the models.

4) The study further reveals that the models' severe deficiencies in simulating the Southeast Asia and WNP monsoon rainfall results from the failure to simulate correctly the relationship between the local rainfall and SST anomalies over the tropical WNP, the South China Sea, and the Bay of Bengal. Over these warm monsoon oceans, the observed summer rainfall anomalies are negatively correlated with local SST anomalies, whereas in nearly all of the models, the rainfall anomalies are positively correlated with local SST anomalies (Table 3).

b. Discussion

It is remarkable that over the tropical WNP and the Bay of Bengal all models tend to produce a positive anomalous SST–rainfall correlation, whereas the observed correlation between local rainfall and SST anomalies is negative (Table 3). Although atmosphere–land interaction could complicate the SST–rainfall relationship over the Bay of Bengal and South China Sea areas, its impacts on the tropical WNP should be small. This region is located within a vast warm pool with a nearly uniform SST background during boreal summer and autumn. The lack of SST gradients could degrade the model's capability in simulating the precipitation climatology (Fig. 2) as well as the anomalies associated with ENSO (Fig. 9a). However, these reasons do not explain the opposite SST–rainfall relationship seen in the model simulations. Why do all of the models have problems in simulating rainfall anomalies in these important monsoon ocean regions?

The model cumulus parameterization schemes contain large uncertainties. In view of the fact, however, that these models have used five different cumulus parameterization schemes [Arakawa–Schubert or its modified version, relaxed Arakawa–Schubert, Betts, moist convective adjustment, and mass flux scheme (Table 1 in Waliser et al. 2002)], the uncertainty in the cumulus parameterization alone can hardly explain the failure of all of the models in these warm monsoon ocean regions.

We propose that the problem arises in the main, not from the deficiencies of the model physics, but from the AMIP experimental design in which the atmosphere is forced to respond passively to the specified SSTs. In reality, the SST and rainfall in the monsoon ocean region interact with each other. Their anomalies tend to be negatively correlated, because the SST anomalies are, to a large extent, a response to monsoon forcing. In a region of an enhanced monsoon, the increased rainfall and cloudiness will tend to reduce the downward solar radiation into the ocean mixed layer, meanwhile, the increased rainfall enhances the monsoon westerly winds, which further enhance the surface evaporation cooling and the entrainment cooling at the mixed layer base. In addition, under the increased precipitation, the surface wind stress normally has a positive vorticity or wind stress curl, which will raise the thermocline through Ekman pumping in the upper ocean. The rising thermocline and enhanced upwelling also tend to decrease SST. These three factors can be expected to lower local SSTs and to result in negative SST anomalies. Likewise, positive SST anomalies often occur in regions of suppressed convection. This explains the observed negative correlation shown in Table 3.

In the model experiments, however, the SST anomalies are given as the local external boundary forcing and the model atmosphere has to passively respond to this forcing. Imagine a positive SST anomaly region in the warm pool where the background SST gradient is small but the total SST exceeds 28°C. Local warming would then tend to lower sea level pressure and enhance low-level moisture convergence due to the SST gradient-induced pressure gradients (Lindzen and Nigam 1987), which in turn would enhance local convection. Convection would not be suppressed because the SST is the cause, not the result, of the atmospheric anomalies in the model experimental design. This explains the positive anomalous SST–rainfall correlation shown in Table 3.

In the AMIP intercomparison, atmospheric anomalies are assumed to be reproducible if the lower boundary conditions are specified. This assumption is valid for the El Niño region and a major portion of the A–AM area, but may not be valid for the summer monsoon over the tropical western North Pacific and the Bay of Bengal. Even with a perfect model, the forced response does not necessarily reproduce observed atmospheric anomalies if it neglects the nonlinear air–sea coupling. Introduction of an interactive ocean is expected to provide a ''delayed'' response and feedback to the atmosphere that can modulate the evolution of the monsoon. In this sense, consideration of the active monsoon–ocean interaction may be necessary for realistic simulation of the Asian summer monsoon. Further study of the nature of the monsoon–ocean interaction may be the key for advancing our understanding of monsoon variability.

It is noted that for the unprecedented strong 1997/98 El Niño episode, the models under study experience unusual difficulties in simulating the Indian monsoon circulation anomalies. Why the models' simulations for the 1997/98 El Niño differ from long-term runs remains an unanswered question.

Acknowledgments. This work is a contribution to the Asian–Australian Monsoon GCM Intercomparison Project initiated by the CLIVAR International Monsoon Panel. The NOAA OGP/Pacific Program and NSF Climate Dynamics Program under Grant ATM00-73023 provided support for the first author. The second and third authors are supported by the Climate Environ-

mental System Research Center at Seoul National University, which is sponsored by the Korea Science and Engineering Foundation and Brain Korea 21. The authors appreciate, the comments of Dr. Speidel and Mr. Ventham, which improved the presentation of this paper. The International Pacific Research Center is in part sponsored by the Frontier Research System for Global Change.

REFERENCES

Angell, J. K., 1981: Comparison of variations in atmospheric quantities with sea surface temperature in the equatorial eastern Pacific. *Mon. Wea. Rev.,* **109,** 230–243.

Gadgil, S., and S. Sajani, 1998: Monsoon precipitation in the AMIP runs. *Climate Dyn.,* **14,** 659–689.

Gates, W. L., and Coauthors, 1999: An overview of the results of the Atmospheric Model Intercomparison Project (AMIPI). *Bull. Amer. Meteor. Soc.,* **80,** 29–55.

Goswami, B. N., 1998: Interannual variations of Indian summer monsoon in a GCM: External conditions versus internal feedbacks. *J. Climate,* **11,** 501–522.

Gruber, A., X. Su, M. Kanamitsu, and J. Schemm, 2000: The comparison of two merged rain gauge–satellite precipitation datasets. *Bull. Amer. Meteor. Soc.,* **81,** 2631–2644.

Kalnay, E., and Coauthors, 1996: The NCEP/NCAR 40-Year Reanalysis Project. *Bull. Amer. Meteor. Soc.,* **77,** 437–471.

Kang, I.-S., and Coauthors, 2002a: Intercomparison of GCM simulated anomalies associated with the 1997–98 El Niño. *J. Climate,* **15,** 2791–2805.

——, and Coauthors, 2002b: Intercomparison of the climatological variations of Asian summer monsoon precipitation simulated by 10 GCMs. *Climate Dyn.,* **19,** 383–395.

Krishnamurti, T. N., C. M. Kishtawal, Z. Zhang, T. E. LaRow, D. R. Bachiochi, C. E. Williford, S. Gadgil, and S. Surendran, 2000: Multimodel ensemble forecasts for weather and seasonal climate. *J. Climate,* **13,** 4196–4216.

Lau, K. M., and H. Weng, 2001: Coherent modes of global SST and summer rainfall over China: An assessment of the regional impacts of the 1997–98 El Niño. *J. Climate,* **14,** 1294–1308.

Lau, N. C., and M. J. Nath, 2000: Impact of ENSO on the variability of the Asian–Australian monsoons as simulated in GCM experiments. *J. Climate,* **13,** 4287–4309.

Liang, X.-Z., W.-C. Wang, and A. N. Samel, 2001: Biases in AMIP model simulations of the east China monsoon system. *Climate Dyn.,* **17,** 291–304.

Lindzen, R. S., and S. Nigam, 1987: On the role of sea surface temperature gradients in forcing low-level winds and convergence in the tropics. *J. Atmos. Sci.,* **44,** 2418–2436.

McBride, J. L., 1987: The Australian summer monsoon. *Monsoon Meteorology,* C.-P. Chang and T. N. Krishnamurti, Eds., Oxford University Press, 203–231.

McPhaden, M. J., 1999: Genesis and evolution of the 1997–98 El Niño. *Science,* **283,** 950–954.

Parthasarathy, B., R. R. Kumar, and D. R. Kothawale, 1992: Indian summer monsoon rainfall indices, 1871–1990. *Meteor. Mag.,* **121,** 174–186.

Rasmusson, E. M., and T. H. Carpenter, 1983: The relationship between eastern equatorial Pacific sea surface temperatures and rainfall over India and Sri Lanka. *Mon. Wea. Rev.,* **111,** 517–528.

Rayner, N. A., E. B. Horton, D. E. Parker, C. K. Folland, and R. B. Hackett, 1996: Version 2.2 of the global sea-ice and sea surface temperature data set, 1903–1994. Climate Research Tech. Note 74, Hadley Centre for Climate Prediction and Research, 35 pp.

Soman, M. K., and J. M. Slingo, 1997: Sensitivity of Asian summer monsoon to aspects of sea surface temperature anomalies in the tropical Pacific Ocean. *Quart. J. Roy. Meteor. Soc.,* **123,** 309–336.

Sperber, K. R., and T. N. Palmer, 1996: Interannual tropical rainfall variability in general circulation model simulations associated with the Atmosphere Model Intercomparison Project. *J. Climate,* **9,** 2727–2750.

Tao, S. Y., and L. X. Chen, 1987: A review of recent research on the East Asia summer monsoon in China. *Monsoon Meteorology,* C. P. Chang and T. N. Krishnamurti, Eds., Oxford University Press, 60–92.

Waliser, D. E., and Coauthors, 2002: AGCM simulations of intraseasonal variability associated with the Asian summer monsoon. *Climate Dyn.,* **21,** 423–446.

Wang, B., and Z. Fan, 1999: Choice of South Asian summer monsoon indices. *Bull. Amer. Meteor. Soc.,* **80,** 629–638.

——, and LinHo, 2002: Rainy season of the Asian–Pacific summer monsoon. *J. Climate,* **15,** 386–398.

——, R. Wu, and X. Fu, 2000: Pacific–East Asian teleconnection: How does ENSO affect East Asian climate? *J. Climate,* **13,** 1517–1536.

——, ——, and K. M. Lau, 2001: Interannual variability of the Asian summer monsoon: Contrasts between the Indian and the western North Pacific–East Asian monsoons. *J. Climate,* **14,** 4073–4090.

Webster, P. J., 1983: The large scale structure of the tropical atmosphere. *Large-Scale Dynamical Processes in the Atmosphere,* B. J. Hoskins and R. P. Pearce, Eds., Academic Press, 235–275.

——, and S. Yang, 1992: Monsoon and ENSO. *Quart. J. Roy. Meteor. Soc.,* **118,** 877–926.

——, V. O. Magana, T. N. Palmer, J. Shukla, R. A. Tomas, M. Yanai, and T. Yasunari, 1998: Monsoons: Processes, predictability, and the prospects for prediction. *J. Geophys. Res.,* **103,** 14 451–14 510.

Wu, M. L. C., S. Schubert, I.-S. Kang, and D. E. Waliser, 2002: Forced and free intraseasonal variability over the south Asian monsoon region simulated by 10 AGCMs. *J. Climate,* **15,** 2862–2880.

Xie, P., and P. A. Arkin, 1997: Global precipitation: A 17-year monthly analysis based on gauge observation, satellite estimates, and numerical model outputs. *Bull. Amer. Meteor. Soc.,* **78,** 2539–2558.

Zhang, Y., and Coauthors, 1997: East Asian winter monsoon: Results from eight AMIP models. *Climate Dyn.,* **13,** 797–820.